

## Broadband tunable operation of compact Yb:CGYA disordered crystal laser

WANG Kang, WU Wen-jie, ZHANG Pei-xiong, YIN Hao, ZHU Si-qi, LI Zhen, CHEN Zhen-qiang

Citation:

WANG Kang, WU Wen-jie, ZHANG Pei-xiong, YIN Hao, ZHU Si-qi, LI Zhen, CHEN Zhen-qiang. Broadband tunable operation of compact Yb:CGYA disordered crystal laser[J]. *Chinese Optics*, 2025, 18(6): 1495–1505. doi: 10.37188/CO.EN-2025-0029

王康, 吴文杰, 张沛雄, 尹浩, 朱思祁, 李真, 陈振强. 紧凑型Yb:CGYA无序晶体激光器的宽带可调谐操作[J]. *中国光学*, 2025, 18(6): 1495–1505. doi: 10.37188/CO.EN-2025-0029

View online: <https://doi.org/10.37188/CO.EN-2025-0029>

### Articles you may be interested in

[Polarization-multiplexing of a laser based on a bulk Yb:CALGO crystal](#)

基于Yb:CALGO晶体激光器的偏振复用

*Chinese Optics*. 2023, 16(6): 1475 <https://doi.org/10.37188/CO.EN-2023-0005>

[Compact pulsed CO<sub>2</sub> laser with wavelength automatic tuning](#)

紧凑型波长自动调谐脉冲CO<sub>2</sub>激光器

*Chinese Optics*. 2022, 15(5): 1007 <https://doi.org/10.37188/CO.2022-0107>

[Writing nanopores on a ZnS crystal with ultrafast Bessel beams](#)

超快贝塞尔光束在硫化锌晶体表面制备纳米孔

*Chinese Optics*. 2021, 14(1): 213 <https://doi.org/10.37188/CO.2020-0101>

[Bandwidth-tunable terahertz metamaterial half-wave plate component](#)

带宽可调谐的太赫兹超构材料半波片器件

*Chinese Optics*. 2023, 16(3): 701 <https://doi.org/10.37188/CO.2022-0198>

[Photonics generation of broadband millimeter wave noise signals with high excess noise ratios](#)

高超噪比宽带毫米波噪声信号光子学产生研究

*Chinese Optics*. 2022, 15(2): 251 <https://doi.org/10.37188/CO.2021-0158>

[Tunable narrowband microwave photonic filter based on brillouin fiber oscillator](#)

基于布里渊光纤振荡器的可调谐窄带微波光子滤波器研究

*Chinese Optics*. 2022, 15(4): 660 <https://doi.org/10.37188/CO.2022-0057>

## Broadband tunable operation of compact Yb:CGYA disordered crystal laser

WANG Kang<sup>1,2,3</sup>, WU Wen-jie<sup>2,3</sup>, ZHANG Pei-xiong<sup>2,3</sup>, YIN Hao<sup>2,3</sup>, ZHU Si-qi<sup>2,3\*</sup>,  
LI Zhen<sup>2,3</sup>, CHEN Zhen-qiang<sup>2,3</sup>

1. *International Collaborative Laboratory of 2D Materials for Optoelectronics Science & Technology, Institute of Microscale Optoelectronics, Shenzhen University, Shenzhen 518060, China;*
2. *Guangdong Provincial Engineering Research Center of Crystal and Laser Technology, Guangzhou 510632, China;*
3. *Department of Optoelectronic Engineering, Jinan University, Guangzhou 510632, China)*

\* *Corresponding author, E-mail: tzhusiqi@jnu.edu.cn*

**Abstract:** A Yb:CaGd<sub>0.33</sub>Y<sub>0.625</sub>AlO<sub>4</sub> (Yb:CGYA) laser crystal of high optical quality has been successfully synthesized via the Czochralski method. The introduction of Gd<sup>3+</sup> ions preserves the original structure and efficiently generates inhomogeneous broadening of the Yb<sup>3+</sup> ion emission spectra. The fluorescence emission peak wavelength of the Yb:CGYA crystal is 1053 nm, and the corresponding measured full width at half-maximum is 93 nm. A tunable laser output ranging from 1017 nm to 1073 nm is achieved by using a bi-refrident filter, which represents the broadest tuning range reported in a short cavity to date. The compact laser offers significant advantages for its applications around the 1 μm wavelength band.

**Key words:** Yb:CGAY; broadband laser; disorder crystal

收稿日期:2025-04-16; 修订日期:2025-05-07

基金项目:国家自然科学基金(No. 12304478, No. 61935010, No. 51972149, No. 51872307, No. 51702124, No. 61975069); 广东省基础与应用基础研究基金(No. 2024A1515012152, No. 2022A1515010326); 广东省重点研发计划(No. 2020B090922006); 广东省科技计划项目(No. 2018B030323017); 广州市科技项目(No. 202206010082, No. 201903010042, No. 201904010294)

Supported by National Natural Science Foundation of China (NSFC) (No. 12304478, No. 61935010, No. 51972149, No. 51872307, No. 51702124, No. 61975069); Guangdong Basic and Applied Basic Research Foundation (No. 2024A1515012152, No. 2022A1515010326); Key-Area Research and Development Program of Guangdong Province (No. 2020B090922006); Guangdong Project of Science and Technology (No. 2018B030323017); Project of Science and Technology of Guangzhou Municipality (No. 202206010082, No. 201903010042, No. 201904010294)

# 紧凑型 Yb:CGYA 无序晶体激光器的 宽带可调谐操作

王康<sup>1,2,3</sup>, 吴文杰<sup>2,3</sup>, 张沛雄<sup>2,3</sup>, 尹浩<sup>2,3</sup>, 朱思祁<sup>2,3\*</sup>, 李真<sup>2,3</sup>, 陈振强<sup>2,3</sup>

(1. 深圳大学微纳光电子学研究院 二维材料光电科技国际合作联合实验室, 广东深圳 518060;

2. 广东省晶体材料和晶体激光技术与应用工程技术研究中心, 广东广州 510632;

3. 暨南大学光电工程系, 广东广州 510632)

**摘要:**利用直拉法成功合成了具有高光学质量的 Yb:CaGd<sub>0.33</sub>Y<sub>0.625</sub>AlO<sub>4</sub> (Yb:CGYA) 激光晶体。引入 Gd<sup>3+</sup>离子有助于保持原始结构, 并有效诱导 Yb<sup>3+</sup>离子发射光谱的非均匀展宽。Yb:CGYA 晶体的荧光发射峰波长为 1053 nm, 对应的半峰全宽为 93 nm。通过使用双折射滤波片实现了从 1017 nm 至 1073 nm 的可调谐激光输出, 这是迄今为止在短腔中报道的最宽调谐范围。这种紧凑型激光器为其在 1 μm 波段附近的应用提供了巨大潜力。

**关键词:** Yb:CGYA; 宽带激光; 无序晶体

中图分类号: TN248.1

文献标志码: A

doi: 10.37188/CO.EN-2025-0029

CSTR: 32171.14.CO.EN-2025-0029

## 1 Introduction

Crystals doped with Yb<sup>3+</sup> ions are commonly utilized for producing 1 μm tunable lasers and mode-locked lasers, attributed to their high quantum efficiency and wide spectral band<sup>[1-4]</sup>. Stark splitting, caused by the two Yb<sup>3+</sup> ions, results in a broad absorption and fluorescence spectrum. The simple energy level structure also ensures low quantum efficiency, avoiding undesirable effects such as excited state absorption and up-conversion<sup>[5-6]</sup>. In the past, the most commonly used Yb<sup>3+</sup>-doped material for generating mode-locked laser pulses was Yb<sup>3+</sup>:Y<sub>3</sub>Al<sub>5</sub>O<sub>12</sub> (Yb:YAG)<sup>[7-9]</sup>. However, the full width at half-maximum (FWHM) of the Yb:YAG crystal's fluorescence emission spectrum is generally about 30 nm<sup>[10-11]</sup>, which largely limits the ability of mode-locked lasers to achieve higher power and narrower laser pulses. To further broaden the spectral band and obtain narrower laser pulses, researchers have developed a series of Yb<sup>3+</sup>-doped disordered crystals. Crystals with disordered structures can provide an inhomogeneous strong crystal field for doping rare-earth ions, effectively broadening the absorption and emission spectra.

Tunable lasers can directly demonstrate the advantages of disordered crystals in this regard and further contribute to the realization of ultrashort pulsed lasers. In 2005, Liu J *et al.* successfully grew Yb<sup>3+</sup>:NaLa (WO<sub>4</sub>)<sub>2</sub> (Yb:NLW) and Yb<sup>3+</sup>:NaLa (MoO<sub>4</sub>)<sub>2</sub> (Yb:NLM) crystals using the Czochralski (CZ) method. A continuous tuning range of 40 nm was obtained in a V-shaped cavity using a Lyot filter<sup>[12]</sup>. In the same year, Jacquemet *et al.* investigated the properties of Yb<sup>3+</sup>:Lu<sub>2</sub>SiO<sub>5</sub> (Yb:LSO) and Yb<sup>3+</sup>:Y<sub>2</sub>SiO<sub>5</sub> (Yb:YSO) disordered crystals. The FWHM of the emission spectrum of Yb:LSO crystals and Yb:YSO crystals is about 2 times wider than normal Yb:YAG crystals<sup>[13]</sup>. Even further, in 2006, Du J *et al.* successfully grew Yb:LYSO disordered crystals by combining the above two crystals, measured the FWHM to be 70 nm, and obtained a wavelength-tuned width of 81 nm by using an SF prism as a tuning tool in a V-cavity<sup>[14]</sup>. Similar disordered crystals, such as Yb:GYSO<sup>[15]</sup>, Yb:GSO<sup>[16]</sup>, and Yb:SSO<sup>[17]</sup> are currently available in the tunable ranges of 59 nm, 120 nm, and 66 nm, respectively, and they are also realized using SF prisms in V-shaped cavities. In particular, the CaY-AlO<sub>4</sub> (CYA) and CaGdAlO<sub>4</sub> (CGA) disordered crystals have attracted considerable attention from

researchers due to their broad emission band and excellent thermal conductivity. Li D ZH *et al.* successfully grew Yb:CYA crystals and investigated the crystal properties in 2011<sup>[18]</sup>. The FWHM of the fluorescence emission spectrum was 77 nm. In 2021, Zhao L N *et al.* successfully achieved a broadly tuned laser output in the 1040~1086 nm (46 nm) using a Yb:CALGO crystal. Tuning elements is birefringent filter (BF)<sup>[19]</sup>. In 2011, Tan W D *et al.* realized laser operation based on Yb:CYA crystals. The laser can be continuously tuned from 1008 nm to 1063 nm<sup>[20]</sup>. In 2016, laser operation of Yb:CALGO pumped with 100 W of pump power was demonstrated and 15 W of laser operation was obtained. Yb:CALGO shows a wide laser tunability range (1010-1085 nm) using a V-shaped cavity<sup>[21]</sup>. These disordered crystals, which are isomorphic to K<sub>2</sub>NiF<sub>4</sub> with similar unit cell parameters, belong to the tetragonal system and the space group I4/mmm<sup>[22-23]</sup>. Structural disorder arises from the random distribution of Ln<sup>3+</sup> (Y<sup>3+</sup> or Gd<sup>3+</sup>) and Ca<sup>2+</sup> cations across a single site (C4v), resulting in a significant broadening of the emission spectrum<sup>[18]</sup>. The absorbance and fluorescence spectrum of a material can be broadened by introducing Gd<sup>3+</sup> ions into Yb:CYA. Di J Q *et al.* proposed the Yb:CaGd<sub>0.1</sub>Y<sub>0.9</sub>AlO<sub>4</sub> disordered crystals in 2018 for the first time<sup>[24]</sup>. This crystal's ratio of Gd<sup>3+</sup> ions and Y<sup>3+</sup> ions is 0.1:0.9, leading to a broad fluorescence emission band with a FWHM of 42 nm. Recently, our group has realized Kerr-lens mode-locked laser output using this type of disordered Yb:CGYA crystals, and the results show that this crystal outperforms the Yb:CYA and Yb:CGA crystals in few-optical cycle pulses generation<sup>[25]</sup>. However, this novel crystal has not yet been realized for wide-tuned laser operation. Although many wide-tuning works with Yb-doped crystals have been reported so far, they are realized in long resonant cavities (v-cavity, x-cavity, etc.), making the laser system more complicated. Furthermore, the long-cavity detuning sensitivity is high and susce-

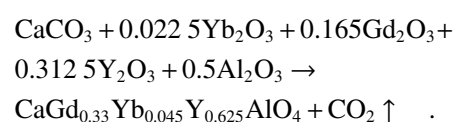
ptible to thermal lensing. Therefore, an in-depth study of tunable lasers based on this crystal is of great importance due to its potential practical applications as a light source and providing a reference candidate for other disordered crystals based on tunable lasers.

In this work, we have successfully grown a 0.45 at. % Yb<sup>3+</sup> doped CaGd<sub>0.33</sub>Y<sub>0.625</sub>AlO<sub>4</sub> mixed crystal with high optical quality by the CZ method. Correspondingly, the emission peak of our crystal is located at 1053 nm. Moreover, a 976 nm LD-pumped Yb:CGYA continuous-wave solid-state laser is demonstrated. Upon supplying a pump power of 16.8 W, we generated a maximum laser output power of 3.7 W, which constitutes a substantial accomplishment. The emission peak of the laser is located at 1049 nm with a FWHM of 10 nm, which owes its breadth to the inclusion of Gd<sup>3+</sup> ions as a dopant, thereby amplifying the system's disorder. The widely wavelength-tunable Yb:CGYA laser with a range of more than 56 nm (from 1017 to 1073 nm) is achieved using a BF, which is the broadest tuning reported so far for short cavities.

## 2 Material and experimental system

### 2.1 Crystal growth

The solid-state reaction method synthesized polycrystalline materials of the Yb<sup>3+</sup> doped Ca(Y, Gd)AlO<sub>4</sub>. The raw materials are CaCO<sub>3</sub>, Gd<sub>2</sub>O<sub>3</sub>, Yb<sub>2</sub>O<sub>3</sub>, Y<sub>2</sub>O<sub>3</sub>, and Al<sub>2</sub>O<sub>3</sub> with purity of 4 N. The corresponding chemical equation is as follows:



The powders are weighed and mixed in a mixer for 36 hours to ensure uniform mixing. The mixed material is pressed into tablets by a press machine. The muffle furnace is used for sintering at 1350 °C.

A high-quality single crystal is grown using the CZ method. The synthesized polycrystalline bulk

material is put into an Ir crucible. Single crystals are grown with the  $\langle 001 \rangle$  oriented  $\text{CaYAlO}_4$  seed crystal under a nitrogen atmosphere. The pulling speed and rotation speed of the seed are set as 0.8–1.2 mm/h and 10–15 rpm. After crystal growth is completed, the crystal is slowly cooled to room temperature at a rate of 40–30 °C h<sup>-1</sup>. The crystal prepared for laser experiments is shown in Fig. 1.

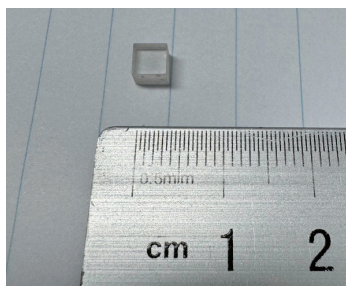


Fig. 1 A photograph of the Yb:CGYA crystal boule. The growth direction is along the  $\langle 001 \rangle$  axis

## 2.2 Laser experiment

The schematic diagram of the Yb:CGYA laser system is shown in Fig. 2(a). The Yb:CGYA crystal measures 4 mm×4 mm×3 mm. The pump source is a fiber-coupled 976 nm laser diode (LD) with a core diameter of 220 μm and a numerical aperture (NA) of 0.22. Two plano-convex lenses, F1 and F2, couple the pump laser into the Yb:CGYA crystal.

Both F1 and F2 are made of K9 glass with a focal length of 50 mm, a radius of curvature of 100 mm and a pump laser transmission of more than 96%. The focus is placed on the surface of the crystal, resulting in a pump beam diameter of 220 μm. To fulfill the conditions for mode-matching between the pump laser and emission laser, the physical res-

onant cavity lengths of 38 mm (CW laser) and 72 mm (CW tunable laser) are designed using the ABCD-matrix formalism. Table 1 lists the relevant optical component parameters used in the experimental setup. Three planar mirrors with different transmittances are used as output-coupled (OC) mirrors, and the transmittances at 1049 nm are 5.7%, 8.4%, and 16.8%, respectively. When tunable laser operation is performed, the resonant cavity length is extended from 38 mm to 72 mm. Based on the existing experimental conditions, a BF with a thickness of 0.05 mm is inserted between the crystal and the OC. The Glan-Taylor Prism is then used for subsequent measurement of the polarization information of the beam. The crystal, wrapped in indium foil, is mounted on a water-cooled copper block and maintained at a temperature of 15 °C. A long-pass filter (Thorlabs, FELH1000) is positioned before the power meter (PM) to eliminate residual pump power. The corresponding physical diagram of the device is shown in Fig. 2(b).

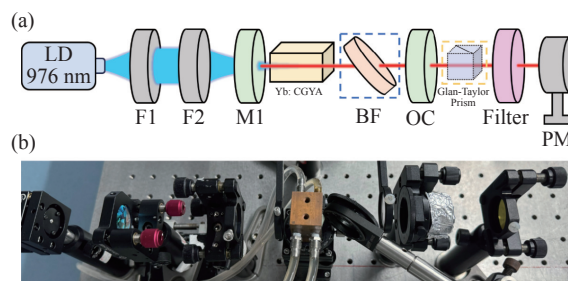


Fig. 2 Experimental set-up diagram. (a) Experiment layouts of the Yb:CGYA laser system; (b) physical drawing of the Yb:CGYA laser system. BF, Bi-refractive filter; PM, Power meter. OC, output-coupled mirror

Tab. 1 Components and parameters in the experimental setup of the Yb:CGYA laser

Component	Parameter
M1	Plano-concave lens, Radius of curvature of 150 mm, Plane coated with anti-reflection film at 980 nm ( $\eta > 90\%$ ), Spherical coated with high-reflection film at 1049 nm ( $\eta > 99.9\%$ ).
OC	M2: Flat mirror, $\eta = 5.7\%$ (1049 nm), Reflectance of 96% at 976 nm. M3: Flat mirror, $\eta = 8.4\%$ (1049 nm), Reflectance of 96% at 976 nm. M4: Flat mirror, $\eta = 16.9\%$ (1049 nm), Reflectance of 85% at 976 nm.
BF	Thickness: 0.05 mm.
Filter	Long-pass filter, Cut-off wavelength at 1000 nm, transmittance below 0.01% in the range of 900 nm to 1000 nm, and transmittance above 97% in 1000 nm to 1100 nm.

### 3 Results and discussion

#### 3.1 Optical properties

The absorption spectrum is recorded with a wavelength range of 300–1000 nm by a Perkin-Elmer UV-Vis-NIR spectrometer (PE Lambda 900). Fluorescence spectra is measured using a Horiba transient QM-8000 fluorescence spectrometer. All measurements are performed at room temperature.

The absorption coefficient spectra of Yb:CGYA crystal at room temperature are shown in Fig. 3.

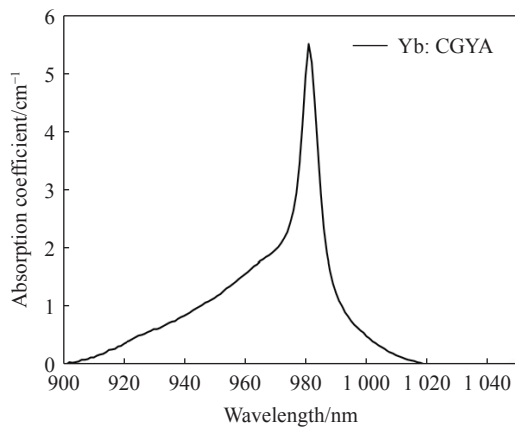


Fig. 3 The absorption coefficient spectra of the Yb:CGYA crystal

The absorption peak at 981 nm belongs to the zero-line transition between the lowest levels of  $^2F_{7/2}$  and  $^2F_{5/2}$  manifolds. It is observed that the absorption coefficient at 981 nm is  $5.5 \text{ cm}^{-1}$  with a FWHM of 7.0 nm. The following formula can be used to calculate the absorption cross-sections:

$$\sigma_{\text{abs}} = \alpha_a / N \quad , \quad (1)$$

where  $\sigma_{\text{abs}}$  represents the absorption cross-section,  $\alpha_a$  is the absorption coefficient, and  $N$  represents the particle number concentration, which can be calculated in the following equation:

$$N = \frac{x\rho DNA}{M} \quad , \quad (2)$$

where  $\rho$ ,  $D$ ,  $NA$ , and  $M$  are the crystal density, doping concentration, Avogadro constant, and the relative molecular weight of the crystal. Then the absorption cross-section at 981 nm is obtained as

$1.47 \times 10^{-20} \text{ cm}^2$  through Equation (2). Broad absorption bands are necessary to increase the diode-pumping efficiency, which shows that the wider absorption band of the Yb:CGYA crystal matches well with the efficient InGaAs laser diode.

Figure 4 shows the emission spectra of the Yb:CGYA crystal. Due to the simple energy level structure of the  $\text{Yb}^{3+}$  ion, the emission spectrum is a single peak. The central wavelength is 1053 nm and its FWHM is 93 nm, which is conducive to fabricating ultrafast and tunable lasers through appropriate experimental facilities.

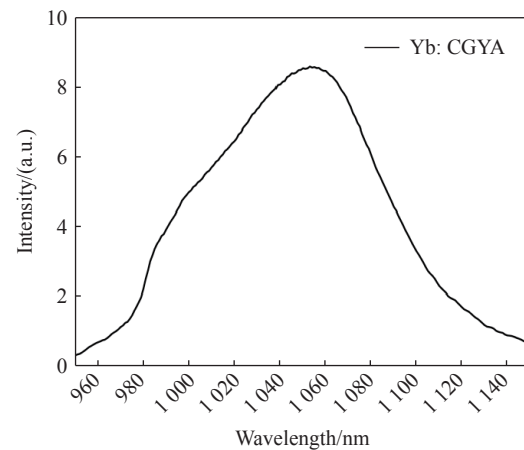


Fig. 4 The emission spectra of the Yb:CGYA crystal

The radiation trap effect of the  $\text{Yb}^{3+}$  ion greatly influences the fluorescence spectrum, making the McCumber method the first choice to calculate the emission cross section from the absorption spectrum. The interaction relationship between the absorption cross section and the emission cross section is as follows:

$$\sigma_{\text{em}}(\lambda) = \sigma_{\text{abs}}(\lambda) \frac{Z_g}{Z_e} \exp((E_{\text{ZL}} - hc\lambda^{-1})/kT) \quad , \quad (3)$$

where  $Z_g$  and  $Z_e$  represent the partition functions of the ground state and the excited state,  $E_{\text{ZL}}$  is the energy difference between the lowest sublevel of the excited state and the ground state, and  $h$ ,  $c$ ,  $\lambda$ ,  $k$  and  $T$  are Planck constant, speed of light, emission wavelength, Boltzmann constant and the thermodynamic temperature. The emission cross section is calculated to be  $0.70 \times 10^{-20} \text{ cm}^2$ .

### 3.2 Laser performance

The stability of the laser cavity is simulated using the resonator software, as shown in Fig. 5 (color online). For a laser system with a cavity length of 38 mm, changes in the focal length of the thermal lens will not cause the system to overflow the stabilization zone. For a laser system with a cavity length of 38 mm, a change in the focal length of the thermal lens does not cause the system to overflow the stabilization zone. When the focal length of the thermal lens is increased from 100 mm to 1000 mm, the fundamental laser spot radius on the front surface of the crystal increases from 137.5  $\mu\text{m}$  to 154  $\mu\text{m}$ , which is slightly smaller than the core radius of the pump source and allows the system to operate better in the TEM<sub>00</sub> mode. However, the minor mode volume of the system is not advantageous for generating a high-power laser. For a laser system with a cavity length of 72 mm, the system's stable operation is ensured when the thermal focal length exceeds 120 mm. When the focal length of the thermal lens is increased from 120 mm to 150 mm, the base laser spot radius of the front surface of the crystal decreases sharply from 406  $\mu\text{m}$  to 242  $\mu\text{m}$ . When it continues to increase from 150 mm to 500 mm, the base laser spot radius of the front surface of the crystal decreases from 242  $\mu\text{m}$  to 201  $\mu\text{m}$ . In the range of 500 mm to 1000 mm, the base laser spot radius of the front surface of the crystal is almost unchanged. The analysis shows that the res-

onant cavity is well designed based on the experimental basic conditions.

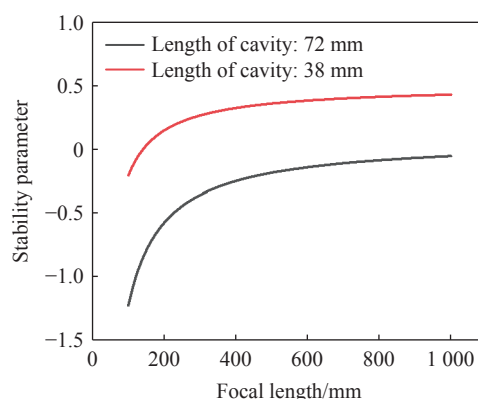


Fig. 5 The relationship between focal length of the thermal lens and the thermal stability of the simulated laser system

When BF and Glan-Taylor Prism are not added and the cavity length is set to 38 mm, the input-output characteristics of the system are investigated in this experiment, as shown in Fig. 6(a) (color online). When the transmittances of the coupling output mirrors are set to 5.7%, 8.4%, and 16.9%, the maximum output powers obtained are 3 W, 3.55 W, and 3.7 W, respectively, and the corresponding slope efficiencies of the linear fits are 25.6%, 30.1% and 34.5%, respectively. The power of the laser depends linearly on the pump power and no saturation is observed. However, the absence of coatings on the crystal and the relatively low doping concentration of Yb<sup>3+</sup> ions (5%) limit the further power increase.

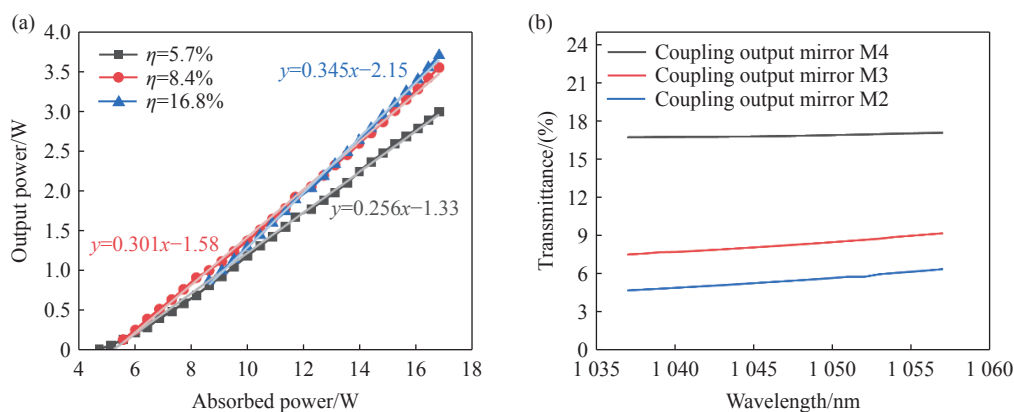


Fig. 6 Laser input-output characteristics of coupled output mirrors with varying transmittances. (a) Output power versus the absorbed pump power; (b) the transmission curve of the M2, M3, and M4 output mirrors within the wavelength range of 1037 nm to 1057 nm

Figure 6(b) (color online) provides the transmittance spectra of coupling output mirrors M2, M3, and M4 in the wavelength range from 1 037 nm to 1 057 nm. The transmittance of the coupling output mirror M2 demonstrates a minimum value of 4.6% at 1 037 nm and a maximum value of 6.3% at 1 057 nm within this range, indicating similar losses across different longitudinal modes within the specified spectral range. The transmittance curves of M3 and M4 coupling output mirrors display a flat profile similar to M2 within the same wavelength range, thus ensuring broadband lasing due to relatively uniform transmittance. The output laser spectrum, measured using a spectrum analyzer (YOKOGAWA AQ6374), is shown in Fig. 7 (color online), with the emission peak of the laser located at 1 049 nm and a FWHM of 10 nm. The mode field of the laser beam is then characterized. As shown in Fig. 8(a) (color online), to prevent damage to the measuring instrument, the laser first passes through the neutral density attenuator, with its power reduced from 3 W to 0.25 W. Then, it is focused onto the CCD camera by a plano-convex lens (F3) with a focal length of 250 mm. The mode field profile follows a typical Gaussian distribution (Fig. 8(b), color online), indicating that the laser operates well in the TEM<sub>00</sub> mode. These results align with our system design.

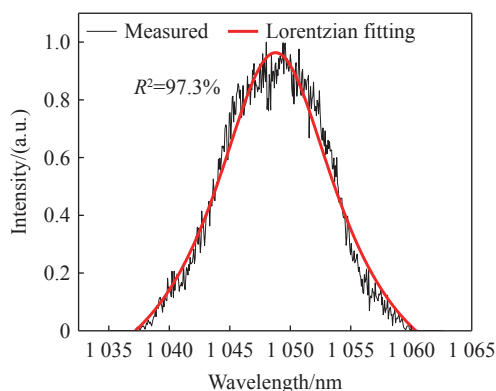


Fig. 7 Measured (black line) and fitted (red line) spectral curve of the laser with transmittance of oc mirror of 5.7%

Subsequently, the power stabilization of the Yb:CGYA laser is monitored, as shown in Fig. 9

(color online). Since the intensity resolution of the power meter is only 10 mW in the range above 2 W, the power stability of the laser power near 2 W output is also measured in addition to the maximum power one. At the maximum absorbed pump power of 16.8 W, the laser output power instability is less than 0.36% and 0.32% for  $\eta_{oc}=5.7\%$  and  $\eta_{oc}=8.4\%$ , respectively. When the pump absorbed power is 11.7 W, the laser output power instability is less than 0.32% and 0.59% for  $\eta_{oc}=5.7\%$  and  $\eta_{oc}=8.4\%$ , respectively. The low volatility can be attributed to the high thermal conductivity of Yb:CGYA crystals.

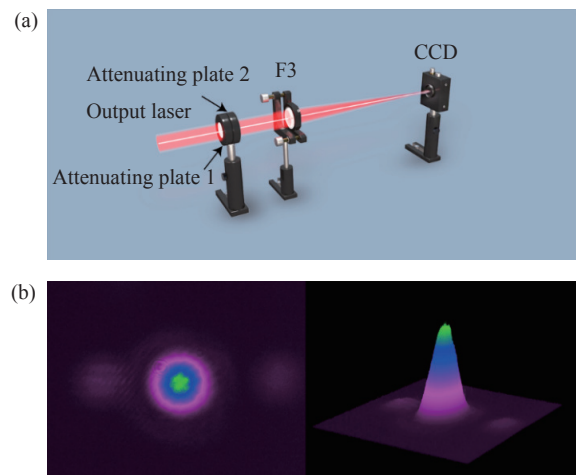


Fig. 8 Laser spot measurement. (a) Measurement device for laser spot profiling; (b) 2-D and 3-D laser beam profiles of the Yb:CGYA laser. F3, planoconvex lens

To further measure the Yb:CGYA crystal's lasing performance and fully demonstrate its great potential for generating ultrashort pulsed lasers, the wavelength tunable performance of the Yb:CGYA laser is measured. The principle of BF is that only light waves meeting half-wave or full-wave phase delays of integer multiples can pass through the quartz crystal at Brewster's angle with minimum loss, shown as follows:

$$\frac{2\pi}{\lambda} \Delta n d = m\pi, m = 0, \pm 1, \pm 2, \pm 3 \dots \quad (4)$$

where  $d$  represents the optical distance through the BF.  $\Delta n$  is the absolute value of the difference between the refractive indices, and the two refract-

ive indices of a light wave in different polarization directions can be found by the Sellmeier formula.

Rotating the BF can change the refractive index difference and thus the output wavelength<sup>[26]</sup>.

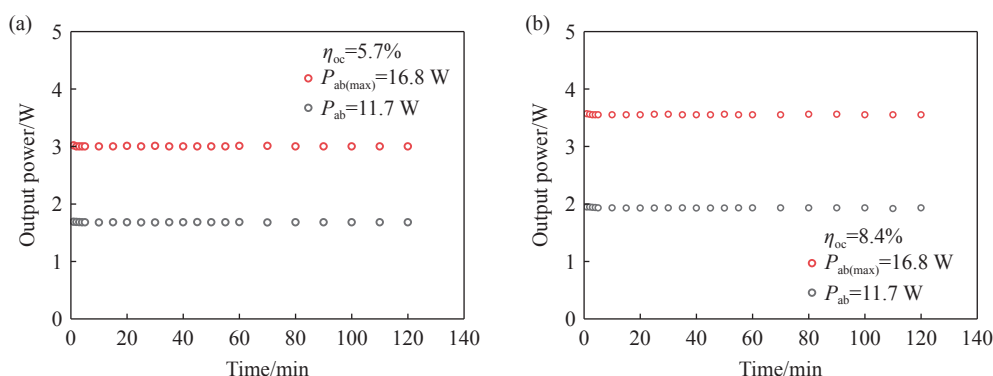


Fig. 9 Yb:CGYA laser stability test results. (a)  $\eta = 5.7\%$  for OC mirror; (b)  $\eta = 8.4\%$  for OC mirror

Setting the cavity length to 72 mm on top of the original, the input-output characteristics of the system are also investigated in this experiment, as shown in Fig. 10 (color online). The difference is that the OC mirror with  $\eta=16.8\%$  is not used because too high a cavity loss would prevent the band at the gain edge from oscillating to produce laser output, which means that the tunable range would be significantly compressed. When the transmittances of the coupling output mirrors are set to 5.7% and 8.4%, the maximum output powers obtained are 1.921 W and 2.430 W, respectively. The corresponding slope efficiencies of the linear fits are measured to be 17.4% and 22.6%, respectively. It was established that extending the resonant cavity led to a marginal deterioration in the output laser performance, yet had no substantial impact on the laser tuning operation.

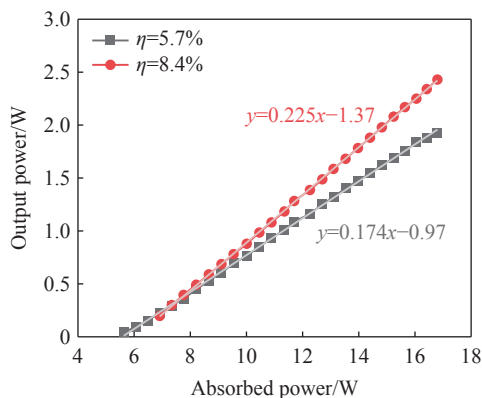


Fig. 10 Laser input-output characteristics of coupled output mirrors using the BF

A Glan-Taylor prism is added in the laser path behind the output coupler to record the polarized characteristics of the tunable Yb:CGYA laser system under its maximum output power. As is shown in Fig. 11 (color online), they are both linearly polarized. The output laser's polarization extinction ratio (PER) is calculated to be 12.41 dB and 16.15 dB for  $\eta_{oc}=5.7\%$  and  $\eta_{oc}=8.4\%$ , respectively. Above characteristics demonstrate that, even though the system is operating at a relatively high absorbed pumped power, the Yb:CGYA crystal can generate a great linearly-polarized laser and has an excellent ability in polarization-maintaining, which is favorable in nonlinear conversion.

For wavelength selection, a 0.05 mm tick BF is placed inside the cavity at the Brewster angle. The wavelength tuning of Yb:CGYA is illustrated in Fig. 12 (color online). To obtain a tuned laser output with sufficient power, OC transmittances of 5.7% and 8.4% are used, and their maximum output laser powers are obtained at the 1049 nm band, which are 1.111 W and 1.894 W. The maximum tuning ranges obtained are 56 nm (from 1017 nm to 1073 nm) and 36 nm (from 1028 nm to 1064 nm), respectively. The wavelength tuning curve of Yb:CGYA is very smooth and has slight fluctuations. For 5.7% transmittance, it sustains a broad range of 20 nm over 1.0 W, from 1037 to 1057 nm. For 8.4% transmittance, it sustains a broad range of

15 nm over 1.5 W, from 1 040 to 1 055 nm. In Addition, the wavelength tuning range is susceptible to the cavity losses. When the  $\eta_{oc}$  is changed from 8.4% to 5.7%, the tuning range is increased by 20 nm, but this is at the expense of a higher-power laser output. Compared with folded cavities, compact straight cavities are more difficult to achieve broad-spectrum tuning due to the larger longitudinal mode spacing. However, the advantages of straight cavities are undeniable, and they overcome the problems of other resonance cavities, such as high detuning sensitivity and large total volume. It is easy for straight cavities to be practically applied. Our results are even wider or comparable to many that use V-cavities to achieve tuning, such as Yb:NLW (40 nm) and Yb:NLM (38 nm)<sup>[12]</sup>, Yb:CYA (55 nm)<sup>[20]</sup>, Yb:GYSO (59 nm)<sup>[15]</sup>, and Yb:SSO (66)<sup>[17]</sup>. Among many tunings using straight cavities, our results are also wider than most, such as Yb:YAG (29 nm)<sup>[27]</sup>, Yb:CALGO (46 nm)<sup>[19]</sup>,

Yb:LuAG (50 nm)<sup>[28]</sup>. If a wider tuning range is desired, like Yb:GdCOB (tuning range of 102 nm). The shorter the resonant cavity length, the fewer the number of longitudinal modes that can be used for gain-starting, and correspondingly the narrower the tuning range. To our knowledge, among Yb-doped crystal materials, the compact straight cavity (72 mm) used in this paper is the shortest known capable of tuning operation. The ability to achieve a wide range of wavelength tuning and a relatively high tuned output laser power in a short cavity is attributed to the relatively wide emission band of the Yb:CGYA crystals and the excellent crystal quality. Fig. 13 (color online) shows the corresponding laser spectra when the BF is rotated to different angles. As can be seen, in addition to the case of single-wavelength output (Fig. 13(a)), there is also the case of multi-wavelength production (Fig. 13(b)). This is because there is more than one wavelength satisfying formula (4) in a given case.

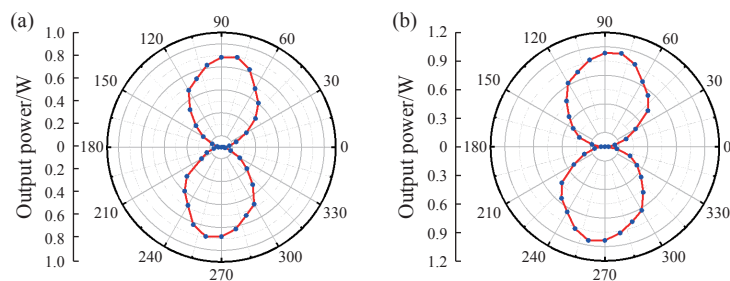


Fig. 11 Polarization measurement of the output laser. (a) Polarization when  $\eta_{oc} = 5.7\%$  of OC. (b) Polarization when  $\eta = 8.4\%$  of OC

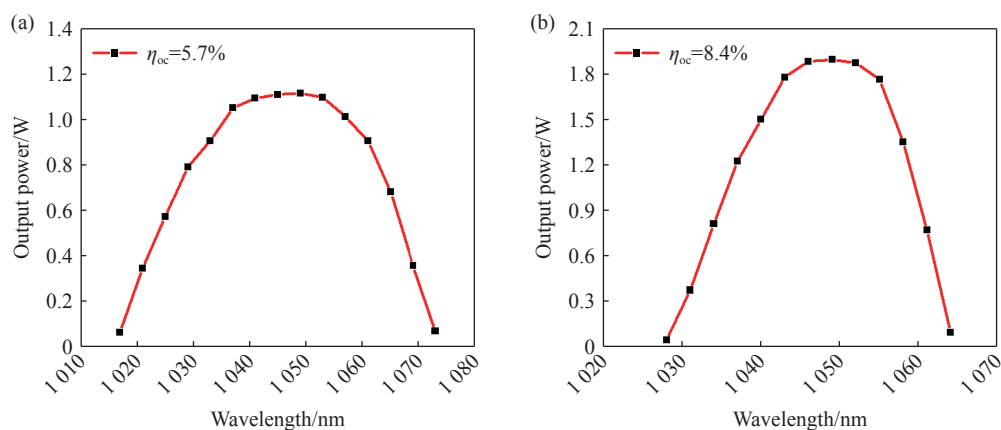


Fig. 12 The laser wavelength tuning curve at an absorption pump power of 16.8 W. (a) The transmittance of the output coupler is 5.7%; (b) The transmittance of the output coupler is 8.4%

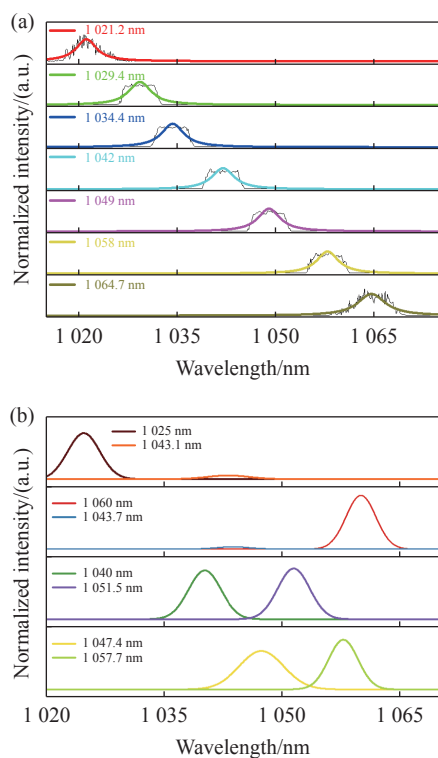


Fig. 13 Spectra of wavelength-tunable operation of Yb:CGYA laser. (a) Single-wavelength operation; (b) multi-wavelength operation

## 4 Conclusion

In summary, we have successfully grown a disordered mixed single crystal of Yb:CGYA using the CZ method. The as-grown crystal's optical proper-

ties and laser performance are investigated in detail. Compared to Yb:CYA crystals, the fluorescence spectrum of Yb<sup>3+</sup> ions exhibits inhomogeneous broadening following the introduction of Gd<sup>3+</sup> ions. The FWHM of the emission spectra of Yb:CGYA crystal at around 1053 nm is 93 nm. To our knowledge, this represents the broadest emission spectrum FWHM for Yb-doped crystalline materials. By conducting continuous-wave laser experiments with Yb:CGYA, we realize a maximum laser power of 3.7 W at a pump power of 16.8 W. The co-doping of Gd<sup>3+</sup> and Y<sup>3+</sup> ions amplifies the disorder within the crystal structure, thereby inducing more significant spectral broadening. Furthermore, the widely wavelength-tunable Yb:CGYA laser with a range of more than 56 nm (from 1017 to 1073 nm) is achieved using a BF. The compact straight cavity (72 mm) used in this work is the shortest known capable of tuning operation. This approach fosters the development of new broad-spectrum crystals, particularly those with disordered structures. It permits substantial spectrum broadening while preserving the original crystal's merits in various respects. Consequently, it is a superior laser material and provides a reference value for studying other disordered crystals and further realizing tunable lasers.

## References:

- [1] TIAN W L, PENG Y N, ZHANG Z Y, *et al.*. Diode-pumped power scalable Kerr-lens mode-locked Yb: CYA laser[J]. *Photonics Research*, 2018, 6(2): 127-131.
- [2] GREBORIO A, GUANDALINI A, AUS DER AU J. Sub-100 fs pulses with 12.5-W from Yb: CALGO based oscillators[J]. *Proceedings of SPIE*, 2012, 8235: 823511.
- [3] DÉLEN X, PIEHLER S, DIDIERJEAN J, *et al.*. 250 W single-crystal fiber Yb: YAG laser[J]. *Optics Letters*, 2012, 37(14): 2898-2900.
- [4] AKBARI R, FEDOROVA K A, RAFAILOV E U, *et al.*. Diode-pumped ultrafast Yb: KGW laser with 56 fs pulses and multi-100 kW peak power based on SESAM and Kerr-lens mode locking[J]. *Applied Physics B*, 2017, 123(4): 123.
- [5] HU Q Q, JIA ZH T, VOLPI A, *et al.*. Crystal growth and spectral broadening of a promising Yb: CaLu<sub>x</sub>Gd<sub>1-x</sub>AlO<sub>4</sub> disordered crystal for ultrafast laser application[J]. *CrystEngComm*, 2017, 19(12): 1643-1647.
- [6] PETIT P O, PETIT J, GOLDNER P, *et al.*. Inhomogeneous broadening of optical transitions in Yb: CaYAlO<sub>4</sub>[J]. *Optical Materials*, 2008, 30(7): 1093-1097.
- [7] ORTAÇ B, SCHMIDT O, SCHREIBER T, *et al.*. High-energy femtosecond Yb-doped dispersion compensation free fiber laser[J]. *Optics Express*, 2007, 15(17): 10725-10732.
- [8] BRUNNER F, PASCHOTTA R, AUS DER AU J, *et al.*. Widely tunable pulse durations from a passively mode-locked thin-disk Yb: YAG laser[J]. *Optics Letters*, 2001, 26(6): 379-381.

- [9] INNERHOFER E, SUDMEYER T, BRUNNER F, *et al.* . 60 W average power in picosecond pulses from a passively mode-locked Yb: YAG thin-disk laser[C]. *Proceedings of the Summaries of Papers Presented at the Lasers and Electro-Optics. CLEO'02. Technical Diges*, IEEE, 2002: 152-153.
- [10] XU X D, ZHAO ZH W, XU J, *et al.*. Crystal growth and spectral properties of Yb<sub>3</sub>Al<sub>5</sub>O<sub>12</sub>[J]. *Journal of Crystal Growth*, 2003, 257(3-4): 272-275.
- [11] BRUESSELBACH H W, SUMIDA D S, REEDER R A, *et al.*. Low-heat high-power scaling using InGaAs-diode-pumped Yb: YAG lasers[J]. *IEEE Journal of Selected Topics in Quantum Electronics*, 1997, 3(1): 105-116.
- [12] LIU J, CANO - TORRES J M, CASCALES C, *et al.*. Growth and continuous - wave laser operation of disordered crystals of Yb<sup>3+</sup>: NaLa(WO<sub>4</sub>)<sub>2</sub> and Yb<sup>3+</sup>: NaLa(MoO<sub>4</sub>)<sub>2</sub>[J]. *Physica Status Solidi (A)*, 2005, 202(4): R29-R31.
- [13] JACQUEMET M, JACQUEMET C, JANEL N, *et al.*. Efficient laser action of Yb: LSO and Yb: YSO oxyorthosilicates crystals under high-power diode-pumping[J]. *Applied Physics B*, 2005, 80(2): 171-176.
- [14] DU J, LIANG X Y, XU Y, *et al.*. Continuous-wave diode-pumped Yb<sup>3+</sup>: LYSO tunable laser[J]. *Proceedings of SPIE*, 2007, 6279: 627963.
- [15] DU J, LIANG X Y, XU Y, *et al.*. Tunable and efficient diode-pumped Yb<sup>3+</sup>: GYSO laser[J]. *Optics Express*, 2006, 14(8): 3333-3338.
- [16] LI W X, HAO Q, ZHAI H, *et al.*. Low-threshold and continuously tunable Yb: Gd<sub>2</sub>SiO<sub>5</sub> laser[J]. *Applied Physics Letters*, 2006, 89(10): 101125.
- [17] ZHANG H Y, LI J F, LIANG X Y, *et al.*. High-power and wavelength tunable diode-pumped continuous wave Yb: SSO laser[J]. *Chinese Optics Letters*, 2012, 10(11): 111404.
- [18] LI D ZH, XU X D, ZHU H M, *et al.*. Characterization of laser crystal Yb: CaYAIO<sub>4</sub>[J]. *Journal of the Optical Society of America B*, 2011, 28(7): 1650-1654.
- [19] ZHAO L N, YUAN Y, TONG L Y, *et al.*. Broadly tunable optical vortex beam in a diode-pumped Yb: CALGO laser[J]. *Optics & Laser Technology*, 2021, 141: 107134.
- [20] TAN W D, TANG D Y, XU X D, *et al.*. Room temperature diode - pumped Yb: CaYAIO<sub>4</sub> laser with near quantum limit slope efficiency[J]. *Laser Physics Letters*, 2011, 8(3): 193-196.
- [21] PETIT P O, GOLDNER P, VIANA B, *et al.*. Diode pumping of Yb<sup>3+</sup>: CaGdAlO<sub>4</sub>[J]. *Proceedings of SPIE*, 2008, 6998: 69980Z.
- [22] KUSTOV E F, PETROV V P, PETROVA D S, *et al.*. Absorption and luminescence spectra of Nd<sup>3+</sup> and Er<sup>3+</sup> ions in monocrystals of CaYAIO<sub>4</sub>[J]. *Physica Status Solidi (A)*, 1977, 41(2): 379-383.
- [23] LAGATSKII A A, KULESHOV N V, SHCHERBITSKII V G, *et al.*. Lasing characteristics of a diode-pumped Nd<sup>3+</sup>: CaGdAlO<sub>4</sub> crystal[J]. *Quantum Electronics*, 1997, 27(1): 15-17.
- [24] DI J Q, SAI Q L, SUN X H, *et al.*. Dual-wavelength and efficient continuous-wave operation of a Yb: CaGd<sub>0.1</sub>Y<sub>0.9</sub>AlO<sub>4</sub> laser[J]. *Laser Physics*, 2018, 28(5): 055803.
- [25] LI ZH Q, LIN ZH L, ZENG H J, *et al.*. Diode-pumped Kerr-lens mode-locked ytterbium-doped compositional mixed calcium aluminate laser[J]. *Optics Express*, 2024, 32(23): 40507-40513.
- [26] ZHAO Z W, HU W J, ZHU S Q, *et al.*. Wide-wavelength-tunable operation of Tm: GYAP disordered crystal laser with birefringence filtering[J]. *Optik*, 2024, 308: 171817.
- [27] TAIRA T, SAIKAWA J, KOBAYASHI T, *et al.*. Diode-pumped tunable Yb: YAG miniature lasers at room temperature: modeling and experiment[J]. *IEEE Journal of Selected Topics in Quantum Electronics*, 1997, 3(1): 100-104.
- [28] BRENIER A, GUYOT Y, CANIBANO H, *et al.*. Growth, spectroscopic, and laser properties of Yb<sup>3+</sup>-doped Lu<sub>3</sub>Al<sub>5</sub>O<sub>12</sub> garnet crystal[J]. *Journal of the Optical Society of America B*, 2006, 23(4): 676-683.

#### Author Biography:



ZHU Si-qi (1985—), Guangdong, Ph.D., Master's Supervisor. The research mainly involves the design of laser systems, laser physics and light-matter interaction. E-mail: [tzhusiqi@jnu.edu.cn](mailto:tzhusiqi@jnu.edu.cn)